ISSN 1054-660X, Laser Physics, 2007, Vol. 17, No. 4, pp. 545–551.

Control of Qubits Encoded in Decoherence-Free Subspaces

P. Cappellaro[a, *], J. S. Hodges[b], T. F. Havel[b], and D. G. Cory[b]

[a] *ITAMP, Harvard-Smithsonian Center for Astrophysics, Cambridge, MA 02138 United States*

[b] *Massachusetts Institute of Technology, Department of Nuclear Science and Engineering, Cambridge, MA 02139 United States*

*e-mail: pcappell@cfa.harvard.edu

Received November 1, 2006

Abstract—Decoherence-free subspaces protect quantum information from the effects of noise that is correlated across the physical qubits used to implement them. Given the ability to impose suitable Hamiltonians upon such a multi-qubit system, one can also implement a set of logical gates which enables universal computation on this information without compromising this protection. Real physical systems, however, seldom come with the correct Hamiltonians built-in, let alone the ability to turn them off and on at will. In the course of our development of quantum information processing devices based on liquid-state NMR, we have found the task of operating on quantum information encoded in decoherence-free subspaces rather more challenging than is commonly assumed. This contribution presents an overview of these challenges and the methods we have developed for overcoming them in practice. These methods promise to be broadly applicable to many of the physical systems proposed for the implementation of quantum information processing devices.

PACS numbers: 03.67.-a, 03.67.Pp, 33.25.+k

DOI: 10.1134/S1054660X0704038X

1. INTRODUCTION

Control of quantum systems, although a challenging task, holds great promise in many emerging physical applications [1]. Schemes to improve the coherent control have been studied [2, 3], while at the same time strategies to protect the quantum system against the effects of the environment have been developed in the context of quantum information processing. Besides active quantum error control codes (QECC) [4, 5], a particularly promising avenue is the passive protection of quantum information via the encoding in noise-invariant subspaces. Decoherence-free subspaces (DFS) [6–8] take advantage of known symmetries of the noise superoperator to individuate degrees of freedom that are invariant under the action of the environment, thus offering an intrinsic protection to information encoded in them. DFS are therefore ideal quantum memories, since contrary to QECC there is no limit to the number of errors they can correct. When one wants to combine coherent control with the protection offered by DFS's, further complications arise due to the constraint that ideally all operations should happen inside a reduced subspace of the total Hilbert space. In this paper, we present some of the challenges that emerge when operating on DFS-encoded qubits and strategies to overcome them. We present a specific instance of a DFS as an example to illustrate much broader issues. With this example at hand, we present in the next section the problem of leakage outside the DFS caused by the real Hamiltonian acting on the system. In Section 3, we show how techniques used to build gates based on average Hamiltonian theory [9] have to be adapted to the presence of noise. With modifications inspired by dynamical decoupling methods [10–12], these schemes can help reducing the deleterious effects of leakage. In Section 4, we analyze the previously introduced technique of strongly modulating pulses (SMP) [13, 14] with respect to the leakage problem. We then combine the two techniques presented to show how they work together to achieve an improved fidelity of the desired gates for encoded qubits.

2. LEAKAGE

Quantum noise acting collectively on two or more qubits may impose symmetries on the bath-system interaction. These, in turn, lead to conserved quantities and in particular subspaces of the system Hilbert space that are invariant under the action of the noise superoperator. If the closed set formed by such conserved quantities is isomorphic to the Pauli operator set, then information can be encoded as logical qubits into these abstract observables [15].

Ideally, the manipulation of quantum information inside a DFS is made possible by applying logical gates, operators that act on logical basis states in the same way as their non-logical analogs. These operators can be defined in terms of the logical basis and, therefore, they respect the symmetries of the encoded subspaces: if the initial state is in the DFS, the final state obtained by applying an ideal logical gate will also be in the DFS.

Consider one of the simplest examples of DFS, a decoherence-free subspace that protects one qubit against collective phase noise, in a four-dimensional Hilbert space [16]. If the noise acts along the z-direc-

tion, the basis states $|0\rangle_L = |01\rangle$ and $|1\rangle_L = |10\rangle$ are immune to the noise ($(\sigma_z^1 + \sigma_z^2)|i\rangle_L = 0$) and, therefore, constitute a DFS. Operators can be defined from this logical basis, for example, we can define the logical identity and logical Pauli matrices:

$$\begin{aligned} \mathbb{1}_L &= (\mathbb{1}^{1,2} - \sigma_z^1\sigma_z^2)/2, \\ \sigma_x^L &= (\sigma_x^1\sigma_x^2 + \sigma_y^1\sigma_y^2)/2, \\ \sigma_y^L &= (\sigma_x^1\sigma_y^2 - \sigma_y^1\sigma_x^2)/2, \\ \sigma_z^L &= (\sigma_z^1 - \sigma_z^2)/2. \end{aligned} \quad (1)$$

By using these operators as generators of the evolution of a logical state (i.e., a state in the DFS), we ensure that the system remains in the DFS.

In experimental implementations of DFS's, however, these operators might not be readily accessible. In general, controlling qubits requires an interplay of the internal and external (control) Hamiltonians in order to obtain the desired propagator. Often, these Hamiltonians do not respect the symmetries of the DFS and they can lead the system outside the protected subspaces. We define as leakage any evolution that causes the system not to be described by a linear combination of the logical basis or, equivalently, any evolution that leads to a nonzero projection onto the non-logical subspaces [17, 18]. Leakage, in turn, will lead to the loss of information at a rate that depends on the noise characteristics, that is, its strength and its correlation time. When one wants to abstract from the details of a particular environment, leakage is, therefore, a good metric to compare different system Hamiltonians with respect to a particular encoding. Only knowledge of the noise spectral density can, however, provide a quantitative measure of the system decoherence time.

For the sake of concreteness, we will refer to the Hamiltonian available in liquid-state NMR to better illustrate the concept of leakage, but the concepts presented are more general and applicable in many situations. In the large magnetic field, weak coupling limit, the internal Hamiltonian governing a pair of homonuclear spins in a molecule is

$$\mathcal{H}_{\text{int}} = \frac{\Delta\omega}{2}(\sigma_z^1 - \sigma_z^2) + \frac{\pi}{2}J\sigma_z^1\sigma_z^2, \quad (2)$$

where $\Delta\omega$ is the chemical shift difference between the two spins, and J is the electron-mediated weak (J–) coupling. Control is obtained by acting on the spins with radio frequency (rf) pulses. In a frame rotating at the same frequency of the RF oscillatory field, the external Hamiltonian (within the RWA) is given by

$$\mathcal{H}_{\text{ext}} = \omega_{\text{rf}}(t)[\cos(\phi)(\sigma_x^1 + \sigma_x^2) + \sin(\phi)(\sigma_y^1 + \sigma_y^2)], \quad (3)$$

where $\omega_{\text{rf}}(t)$ and $\phi(t)$ are controllable by the experimenter.

If we consider again the DFS example presented above, we can observe that the internal Hamiltonian corresponds to a σ_z rotation in the logical basis, while the external Hamiltonian cannot be written in terms of logical operators and, therefore, causes leakage. Since the control Hamiltonian is needed to operate on the system and obtain logical single qubit rotations, leakage is unavoidable.

If, for example, we wanted to perform the equivalent of a spin echo experiment [19] to refocus the evolution given by the internal Hamiltonian, we would need to apply a logical π pulse about σ_x. The ideal operation does not cause leakage since it connects two states in the DFS. We notice, furthermore, that this rotation could be implemented by an ideal RF pulse applied collectively on the two spins, since $P_x(\pi) = e^{-i\pi/2(\sigma_x^1 + \sigma_x^2)} = -e^{-i\pi/2(\sigma_x^1\sigma_x^2)}$, which is equivalent to a π pulse around σ_x^L. Experimentally, this rotation requires the external RF field to be applied for a finite amount of time t_{p}, during which leakage occurs.

Figure 1 illustrates the system trajectory in and out of the protected subspace during the pulse time for a typical initial state $\rho_0 = \sigma_z^L$ (notice that here and in the following we consider only the traceless part of the density matrix, since it is the only part that gives rise to the NMR signal). In this figure, we plot the purity of the system projection on the logical subspace during its evolution under the internal and external Hamiltonians. Defining the projection operator onto the logical subspace as P_L, we plot $P(t) = \text{Tr}[(P_L\rho(t))^2]/\text{Tr}(\rho(t)^2)$ for $\vartheta = 0 \longrightarrow \pi$ ($t = 0 \longrightarrow t_{\text{p}}$), where

$$\hat{\rho}(t) = \exp(-it(\hat{H}_{\text{int}} + \omega_{\text{rf}}(\hat{\sigma}_x^1 + \hat{\sigma}_x^2)) - t\Gamma/T_2)\hat{\sigma}_z^L. \quad (4)$$

Here, we indicate superoperators in the Liouville space by $\hat{}$ and $\Gamma = (\hat{\sigma}_z^1 + \hat{\sigma}_z^2)$ is the noise supergenerator. In the limit of very high RF power $\left(\frac{\Delta\omega}{\omega_{\text{rf}}} \longrightarrow 0\right)$, the system undergoes a π pulse in a time $t_{\text{p}} = \frac{\pi}{\omega_{\text{rf}}}$ and returns completely to the subspace after this time, remaining outside the subspace only for the duration of the pulse. If the ratio $\frac{\Delta\omega}{\omega_{\text{rf}}}$ is nonzero, as actually required for universal control, the return to the logical subspace is imperfect even in the absence of noise. For ω_{rf} which are physically relevant ($\omega_{\text{rf}} < 2\pi 100$ kHz and $0 < \Delta\omega < 2\pi 20$ kHz), a single RF pulse does not result in a logical π rotation due to off-resonance effects. A logical π pulse using a single period of RF modulation is not possible; a more complex RF modulation, like composite pulses [20], strongly-modulating pulses [13, 14], or

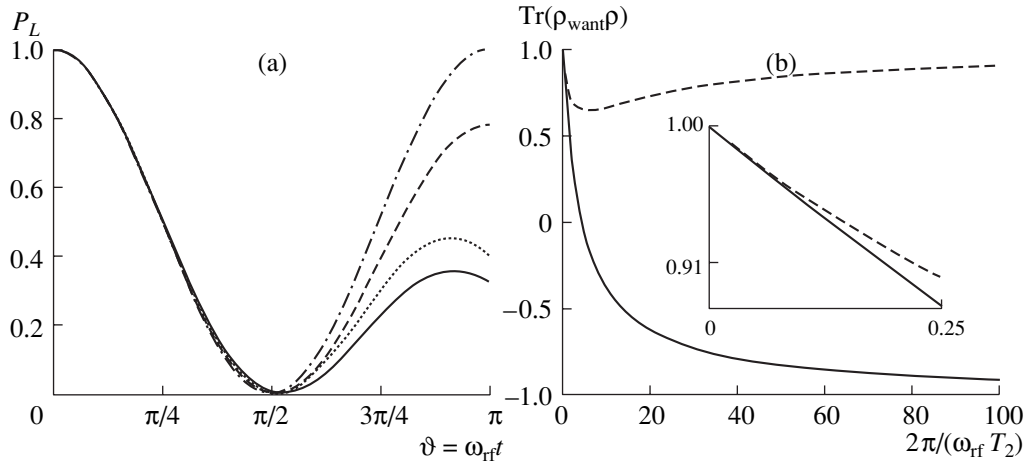

Fig. 1. (a) Projection onto the logical subspace of a state initially inside the DFS, during application of an RF pulse implementing a π rotation about the x axis (see text). The dotted and dash-dotted lines are in the absence of noise, while for the solid and dashed lines a dephasing noise with $T_2 = 4t_p$ was applied. The upper curves (dash-dotted and dashed lines) are for both spins on resonance (chemical shift $\Delta\omega = 0$), while the lower curves (solid and dotted lines) are for a chemical shift $\Delta\omega = 4$ kHz. In the simulations $t_p =$ 111 μs, $J = 40$ Hz and the initial state of the system is σ_z^L. (b) Loss of fidelity due to collective dephasing noise. The desired operation is a collective π rotation of the qubits around the x axis. The plot shows the correlation with the desired state as a function of the inverse product of the RF power ω_{rf} and the relaxation time T_2 for the initial states σ_x^L, $\mathbb{1}_L$ (dashed line) and σ_y^L, σ_z^L (solid line).

optimal control theory [21], is required and will be analyzed in Section 4. Furthermore, if we add the dephasing noise to our simple model, we see that the rotation efficiency is eroded further (lower curves) and it is not possible to bring back the system entirely to the protected subspace since it decays due to decoherence.

This decay depends on the noise strength, in particular, on T_2. This is apparent in Fig. 1b, where we show the correlation loss during a π pulse as a function of the ratio of relaxation time T_2 to pulse time $t_p = \pi/\omega_{rf}$. Notice how for very strong noise, the external control is not able to steer the system from its initial state (hence, the correlation improves for $\rho_0 = \sigma_x^L$, $\mathbb{1}_L$ while it goes to –1 for $\rho_0 = \sigma_z^L$, σ_y^L). In the opposite limit of strong control fields (fast rotations with respect to the decoherence time), the fidelity of single qubit rotations is quite high, as shown in the insets of Fig. 1b. This regime can be reached in liquid state NMR, where nonselective RF pulses can be performed in a few microseconds, compared to T_2 times of milliseconds. However, more complex operations involving, for example, interactions among qubits or selective rotations are expected to require longer times.

In particular, when a complex operation has to be performed on a subset of the qubits, decoupling techniques have to be applied to refocus the evolution of all the other qubits. We now present two complementary strategies to achieve this goal focusing on the challenges they induce when operating with logical qubits and ways to overcome these difficulties.

3. PULSE SEQUENCES FOR NOISE MODULATION

Quantum gates (or any unitary operation) are created by the interplay of the internal and external Hamiltonian (Eqs. (2) and (3)). Specifically, the control Hamiltonian given by the RF fields can be switched on for short periods of time, with varying duration, power, phase, and frequency, in a sequence of pulses and delays. While some control sequences can be found numerically, analytical methods are best suited to provide a systematic method for finding pulse sequences (that can be later optimized numerically). In the NMR tradition, average Hamiltonian theory (AHT) [9] has been used to describe the unitary evolution arising from periodical and cyclic control sequences. The evolution given by time dependent Hamiltonians is expressed in terms of an effective average Hamiltonian

$$U(t_c) = \mathcal{T}\exp\left(-i\int_0^{t_c}\mathcal{H}(t)dt\right) = \exp(-i\overline{\mathcal{H}}t_c), \quad (5)$$

where $\mathcal{T}$ is the Dyson time ordering operator and $\overline{\mathcal{H}}$ the effective Hamiltonian over the control sequence time t_c. For periodical and cyclic control sequences, it is possible to approximate with a high degree of accuracy the effective Hamiltonian with its first terms in the Magnus expansion

$$\overline{\mathcal{H}} \approx \frac{1}{t_c}\int_0^{t_c}\mathcal{H}(t)dt - \frac{i}{2t_c}\int_0^{t_c}dt\int_0^{t}dt'[\mathcal{H}(t),\mathcal{H}(t')] + \ldots. \quad (6)$$

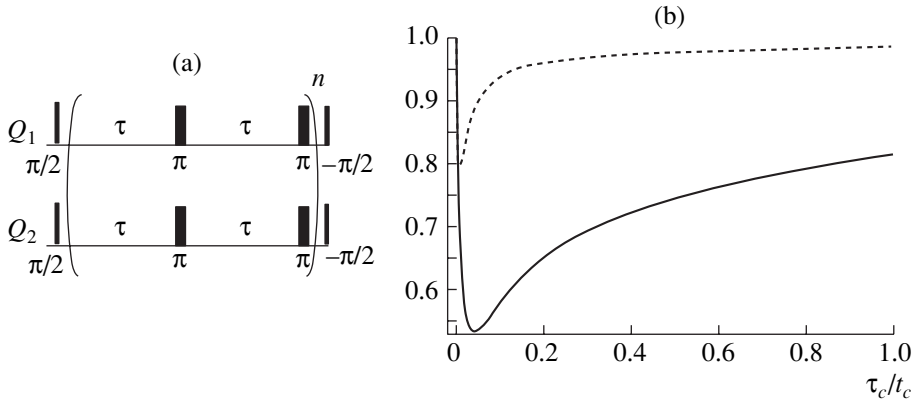

Fig. 2. (a) Pulse sequence to create the logical σ_x^L gate. π pulses are inserted to refocus the unwanted evolution given by the chemical shift term $\frac{\Delta\omega}{2}(\sigma_z^1 + \sigma_z^2)$. The number of π pulses can be increased to reduce the effects of the noise on the system (see text). (b) Fidelity of a π/2 rotation about the logical σ_x^L axis, obtained by the pulse sequence in Fig. 2a for $n = 4$ (solid line) and $n = 16$ (dashed line). The noise strength Ω was fixed at 1 Hz, while the duration of the entire sequence was $t_{\text{tot}} = 2n\tau = 4$ s. We observe an improvement of the fidelity for correlation times longer than the cycle time t_c and a much better performance as more π pulses are introduced. We also notice an increase in fidelity at very short correlation times, which is due to phase fluctuations so fast that they cannot have any effect at the given noise strength.

Considering only the leading term in this expansion, the imposed evolution becomes easy to predict and, conversely, one can build control sequences that implement to first order the desired gate (taking into account higher orders, for example, using simplifications due to symmetries or by numerical optimizations, allows one to devise control sequences that in principle create the desired gate to any order).

AHT is particularly suited for decoupling and refocusing sequences, as well as two-qubit gates. For example, consider the two-qubit DFS introduced previously. In order to implement a rotation about the logical x axis, a two-body interaction must be used. The J-coupling term of the internal Hamiltonian $\frac{\pi}{2}J\sigma_z^1\sigma_z^2$ is rotated to the transverse plane to obtain $\frac{\pi}{2}J\sigma_x^1\sigma_x^2$, and the system is left to evolve for a time $t = 1/2J$. Since, however, the two spins are also evolving under the chemical shift term, one has to cancel out this evolution by inserting, for example, a collective π pulse in the middle of the evolution (see Fig. 2a, where a second π pulse is inserted to make the sequence cyclic).

This control sequence takes the system outside of the protected subspace for a finite amount of time (and given the strength of the J-coupling, usually quite a longer time than for single-qubit rotations). This is a usual drawback for sequences constructed in this way since AHT considers only the average evolution without taking into account the instantaneous trajectory of the system.

When constructing gates, it is, thus, important to use AHT extension to nonunitary evolution (average Liouvillian theory [22, 23]) to also try to refocus at best the noise. Stochastic Liouville theory calculates the evolution of a system in the presence of a random interaction in terms of a cumulant expansion [24]. Using this tool, one can devise modulation schemes that reduce the effects of the noise when the system is brought outside the protected subspace to implement the desired gate via the available control Hamiltonians, thus, combining dynamic decoupling [10–12] with passive noise protection.

Consider, for example, the sequence proposed for the implementation of the logical σ_x^L rotation. If one increases the number of π pulses applied while the system is outside the DFS, the noise effects are much decreased, provided one can reach the regime where the time τ between π pulses becomes smaller than the correlation time τ_c of the noise itself. By calculating the cumulant expansion [24], assuming a Gaussian noise with autocorrelation $G(\tau) = \Omega^2 e^{-\tau/\tau_c}$ and instantaneous ideal pulses, one can find that the fidelity of the system evolution with respect to the desired rotation, $F = \text{Tr}[UU_{\text{want}}^{\dagger}]$ [16, 25], is a function of the number of π pulses applied $2n$ and the interval between them $\tau = t_c/2n$:

$$\begin{aligned} F(\zeta) &= \text{Tr}[\exp(-\Gamma_x^2\zeta(2n\tau)^2/2)] \\ &= \frac{1}{8}(3 + 4e^{-2\zeta n^2\tau^2} + e^{-8\zeta n^2\tau^2}), \end{aligned} \tag{7}$$

where Γ_x is the noise supergenerator Γ rotated along the x axis and

$$\zeta = \frac{2\Omega^2\tau_c^2}{(2n\tau)^2}\Bigg[2n(\tau/\tau_c + e^{-\tau/\tau_c} - 1) + \left(\frac{1-e^{-\tau/\tau_c}}{1+e^{-\tau/\tau_c}}\right)^2 (1 - 2n(1+e^{-\tau/\tau_c}) - e^{-2n\tau/\tau_c})\Bigg]. \quad (8)$$

The fidelity for the logical σ_x^L rotation is plotted in Fig. 2b for 8 and 32 π pulses (corresponding to $n = 4$ and 16 cycles, respectively). As expected, it shows an improvement for a higher number of π pulses and shorter time spacings with respect to the correlation time. Equation (7) and Fig. 2b show the importance of the knowledge of the noise correlation time (and, in general, its spectral density) in designing control sequences for logical qubits, since one must know τ_c to determine the spacing between pulses.

4. STRONGLY MODULATING PULSES

While analytical tools can be helpful for finding many-qubit pulse sequences, a numerical search to build quantum gates is particularly suited for finding single-spin rotations in the presence of other spins when the control field acts on all the spin systems. To obtain the desired selectivity, NMR traditionally relied on low power pulses to address individual spins, but this comes at the cost of long pulse times. A better strategy is to modulate the entire spin system strongly (that is, at a rate fast compared to the spin precession frequencies and the strongest interaction among them) with a modulation that is the result of a numerical search. The modulation is searched by varying the control parameters (intensity ω_{rf}, phase ϕ, and transmitter frequency ω_t) with respect to the maximization of the fidelity between the simulated unitary evolution and the desired gate. Because the characteristic of the pulses found in this way is the strength of the modulation they impose compared to low power selective pulses, they are called strongly modulating pulses (SMP [13, 14]).

Since the numerical search only compares the final unitary operator, disregarding the instantaneous evolution, the system can follow an arbitrary trajectory during the pulse time and, thus, leave the protected subspace. It is interesting to study how these pulses perform with respect to leakage and noise, since the fast and strong modulation itself can constitute an advantage compared to the usual *square* pulses (i.e., pulses with fixed intensity, phase, and frequency).

Figure 3 shows the trajectory in the DFS of a two-spin system during evolution driven by a characteristic strongly modulating pulse. As we can see, this trajectory is more complex than for a square pulse. Furthermore, this yields not only a higher accuracy of the pulse even in the presence of a chemical shift difference between the spins, but also a better performance in a noisy environment, since on the one hand, the system stays closer to the DFS, and on the other hand, the noise itself is partially refocused by the strong modulation. The pulse found was composed of only three intervals with different RF intensity, phase, and frequency because of the simplicity of the system. For larger systems, the modulation is more complex [14], but we expect similar results for the gate fidelity in the presence of noise.

We have further combined the two strategies described for finding quantum gates, that is, pulse sequences designed by AHT, where single pulses are numerically found SMP (the time intervals can be further optimized numerically). We were able to find in this way a good solution to the σ_x^L gate for the DFS under consideration, in particular for noise correlation times longer than the shortest delay possible between pulses. We have studied the accuracy of the gate by numerical simulations, for different values of the noise correlation time. These simulations included the internal Hamiltonian, the external control Hamiltonian, and totally correlated noise $\omega_N(t)(\sigma_z^1 + \sigma_z^2)$ with a stationary Gaussian distribution. The evolution was discretized into equal time steps, for each of which we calculated the propagator $U(t_k) = \exp(-i(H_{int} + H_{ext}(t_k) + \omega(t_k)(\sigma_z^1 + \sigma_z^2))\delta t)$. The noise strength $\omega_N(t_k)$ is extracted from a multivariate Gaussian probability distribution with a covariance matrix $C_{j,k} = \Omega^2 e^{-|j-k|\delta t/\tau_c}$, where j and k are integers indicating the time intervals. We then take the average of the superoperators $S_i = \overline{U}_i \otimes U_i$ obtained over a sequence of evolutions differing only by the random number seed. We have performed simulations using a fictitious two-spin molecule (chemical shift difference $\Delta\omega = 600$ Hz, scalar coupling $J = 50$ Hz), first with instantaneous ideal pulses, then with square pulses (π-pulse time $t_p = 2$ μs), and finally with strongly modulating pulses.

The fidelities of these simulations are plotted as a function of correlation time in Fig. 4. Compared to simulations with ideal pulses, we observe a drop in the fidelity due to the finite duration of each SMP. This drop is only in part accounted for by the increase in time in the cycle length (notice that we kept constant in all the simulations the total sequence time, not the τ spacing between pulses). SMP appear to perform better than the square pulses even if they require longer times, and this advantage will be tantamount in cases where SMP are required because of selectivity issues. The effectiveness of the modulation sequence combined with SMP in preventing decoherence during the unavoidable excursions from the DFS is evident.

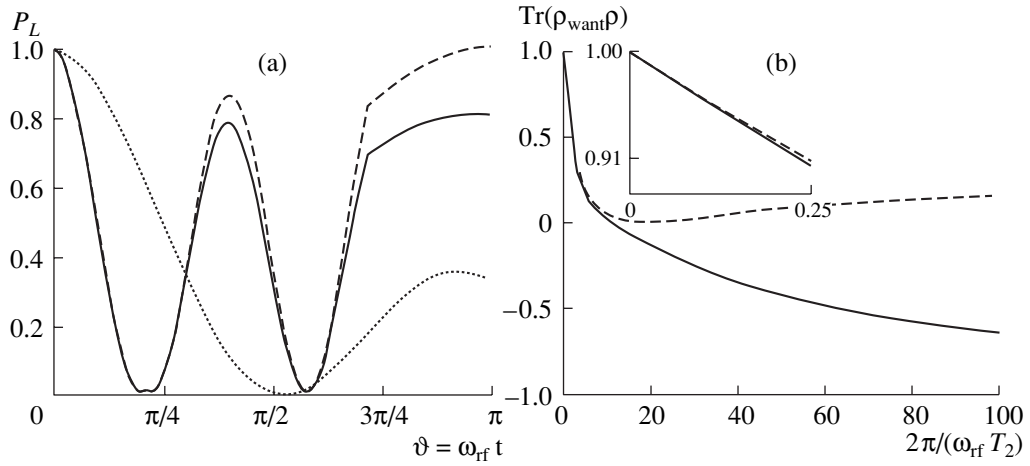

Fig. 3. (a) Projection onto the logical subspace of a state initially inside the DFS during application of an SMP pulse implementing a π rotation about the x axis. The pulse is an example of strongly modulating pulse, with pulse time $t_p = 111$ μs and maximum power $\omega_{rf} = 12$ kHz. The upper curve (dashed line) is in the absence of noise, while for the lower curve (solid line) a dephasing noise with $T_2 = 4t_p$ was applied. In the simulations, the chemical shift is $\Delta\omega = 4$ kHz, $J = 40$ Hz and the initial state of the system is σ_z^L. For comparison, we also plotted the result of a square pulse applied to the same system as already shown in Fig. 1a (dotted line). (b) Loss of fidelity due to collective dephasing noise during a π rotation around the x axis obtained with a strongly modulating pulse. The plot shows the correlation with the desired state as a function of the inverse product of the RF power ω_{rf} and the relaxation time T_2, for the initial states σ_x^L, $\mathbb{1}_L$ (dashed line) and σ_y^L, σ_z^L (solid line). The SMP pulse and system are the same as those defined for Fig. 3a. In the inset, the behavior for strong power and low noise as normally observed in NMR is shown.

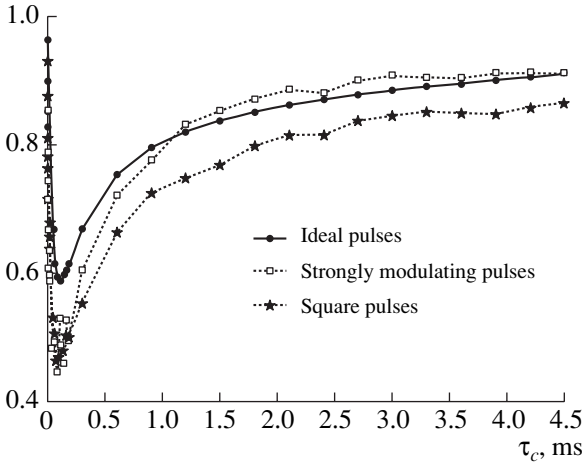

Fig. 4. Fidelity of a $\pi/2$ rotation about the logical σ_x^L axis obtained by the sequence in Fig. 2a with $n = 16$ cycles, where the pulses were ideal pulses (solid line), SMP (squares), and square pulses (stars). Simulations for a two-spin system with chemical shift difference $\Delta\omega = 600$ Hz and scalar coupling $J = 50$ Hz. The noise strength was $\omega_N = 1$ kHz and the cycle time $t_c = 0.82$ ms was kept constant for the three simulations (hence, the interval between pulses τ was varied to accommodate the different lengths of ideal, square, and strongly modulating pulses).

5. CONCLUSIONS

In this paper, we have considered the challenges of operating on quantum information stored in encoded qubits, focusing in particular on the constraints imposed by naturally encountered Hamiltonians that do not provide the logical operation generators. For the sake of concreteness, we presented results relative to the Hamiltonians and control fields specific to liquid state NMR, but we expect that similar difficulties will be encountered in other experimental realizations of quantum information processing, including superconducting qubits, ion traps, and quantum optics. We showed how established methods for finding gates must be modified to take into account the instantaneous evolution of the system that can leak out of the protected subspace. We described general strategies that when combined provide a method for the construction of quantum gates, and we showed numerical results relative to realistic conditions in an NMR experimental implementation which build on and confirm the previously reported results for non-encoded qubits.

In particular, our results emphasize the beneficial role of dynamic decoupling and the fast and strong modulation of SMP to inhibit decoherence during these excursions outside the encoded subspace. This approach depends on the ability to operate on the system on time scales short compared to the correlation time of the noise. These results stress the importance of

characterizing not only the decoherence rate, but also the spectral density of the underlying noise when evaluating various possible realizations of quantum information processing.

ACKNOWLEDGMENTS

This work was supported in part by the National Security Agency (NSA) under Army Research Office (ARO) contract numbers W911NF-05-1-0469 and DAAD19-01-1-0519, by the Air Force Office of Scientific Research, and by the Quantum Technologies Group of the Cambridge-MIT Institute.

REFERENCES

1. I. Chuang and M. A. Nielsen, *Quantum Computation and Quantum Information* (Cambridge Univ. Press, Cambridge, 2000).
2. N. Khaneja, R. Brockett, and S. J. Glaser, Phys. Rev. A **63**, 032308 (2001).
3. J. Botina, H. Rabitz, and N. Rahman, J. Chem. Phys. **104**, 4031 (1996).
4. P. W. Shor, Phys. Rev. A **52**, 2493 (1995).
5. A. R. Calderbank and P. W. Shor, Phys. Rev. A **54**, 1098 (1996).
6. P. Zanardi and M. Rasetti, Phys. Rev. Lett. **79**, 17 (1997).
7. L.-M. Duan and G.-C. Guo, Phys. Rev. Lett. **79**, 1953 (1997).
8. D. A. Lidar, I. L. Chuang, and K. B. Whaley, Phys. Rev. Lett. **81**, 2594 (1998).
9. U. Haeberlen, *High Resolution NMR in Solids: Selective Averaging* (Academic Press, New York, 1976).
10. L. Viola, E. Knill, and S. Lloyd, Phys. Rev. Lett. **82**, 2417 (1999).
11. L. Viola and E. Knill, Phys. Rev. Lett. **90**, 037901 (2003).
12. K. Khodjasteh and D. A. Lidar, Phys. Rev. Lett. **95**, 180501 (2005).
13. E. Fortunato et al., J. Chem. Phys. **116**, 7599 (2002).
14. M. A. Pravia et al., J. Chem. Phys. **119**, 9993 (2003).
15. L. Viola, E. Knill, and R. Laflamme, J. Phys. A **34**, 7076 (2001).
16. E. Fortunato, L. Viola, J. Hodges, et al., New J. Phys **4**, 5 (2002).
17. L. Tian and S. Lloyd, Phys. Rev. A **62**, 050301 (2000).
18. L.-A. Wu, M. S. Byrd, and D. A. Lidar, Phys. Rev. Lett. **89**, 127901 (2002).
19. E. Hahn, Phys. Rev. **80**, 580 (1950).
20. M. Levitt, Prog. Nucl. Magn. Reson. Spectrosc. **18**, 61 (1986).
21. N. Khaneja, T. Reiss, C. Kehlet, et al., J. Magn. Res. **172**, 296 (2005).
22. R. Ghose, Conc. Magn. Res. **12**, 152 (2000).
23. Y. C. Cheng and R. J. Silbey, Phys. Rev. A **69**, 052325 (2004).
24. P. Cappellaro, J. Hodges, T. Havel, and D. Cory, J. Chem. Phys. **125**, 44514 (2006).
25. M. Nielsen, Phys. Lett. A **303**, 249 (2002).